Effect of Cavitation on the Plastic Deformation and Failure of Isotactic Polypropylene

Bing Na, Ruihua Lv

Department of Materials Science and Engineering, East China Institute of Technology, Fuzhou 344000, People's Republic of China

Received 15 January 2007; accepted 28 February 2007
DOI 10.1002/app.26594
Published online 24 May 2007 in Wiley InterScience (www.interscience.wiley.com).

ABSTRACT: To clarify the effect of cavitation, which is mostly induced by crystalline phase, on the plastic deformation and failure of isotactic polypropylene, solid-state annealing at 160°C for 1.5 h is adopted to change the crystalline phase only while the amorphous phase keeps nearly intact. With aid of a special video setup, the relation of true stress and strain as well as the evolution of volume strain with axial strain has been derived. Enhancing crystalline phase due to annealing increases the yield stress and volume strain simultaneously. Moreover, the strain corresponding to steep increasing of volume strain is comparable with that related to yield, indicating that cavitation at early stage is accompanied with process of yield. With knowledge of toughness derived from impact tensile stretching and essential work of fracture (EWF), respectively, the relationship between cavitation and toughness has been correlated to some degree. © 2007 Wiley Periodicals, Inc. J Appl Polym Sci 105: 3274–3279, 2007

Key words: cavitation; isotactic polypropylene; plastic deformation; failure

INTRODUCTION

As in most semicrystalline polymers, tensile deformation of isotactic polypropylene can induce macroscopic whitening.[1–4] It originates from noncohesive damage mechanisms,[5] namely cavitation at microscopic scale, which has been investigated by density measurement, electron microscopy, and small angle X-ray scattering (SAXS). It is well demonstrated that the underlying mechanism of cavitation is related to the misfit of mechanical properties between crystalline and amorphous phase in such a heterogeneous systems. Moreover, cavitation depends on the competition between yield stress of lamellae and negative pressure generated by normal stress in tension.[2] The cavitation during tensile deformation can be observed only when a negative pressure higher than that required for cavitation is present.

$$\sigma/3 = -p > -p_{\mathrm{cav}} \tag{1}$$

where p is the negative pressure generated and p_{cav} is the negative pressure required for cavitation. In the system of isotactic polypropylene with high crystallinity, eq. (1) always holds true and thus cavitation is prevalent, especially at room temperature. In some senses, cavitation can affect the plastic deformation and failure of isotactic polypropylene. Actually, in the literature, improvement of toughness is qualitatively related to the void formation due to stress state conversion.[1] However, the results are based on several polymer grades with distinct chain characteristics, such as molecular weight and isotacticity. It is well known that while isotactic polypropylene crystallizes from melt, different chain characteristics can result in simultaneous change of crystalline and amorphous phase. Therefore, strictly speaking, void-induced toughening in isotactic polypropylene is debatable. On the other hand, though the plastic deformation of isotactic polypropylene has been investigated to a large extent especially by construction of true stress strain curve with aid of special setups,[6,7] the effect of cavitation on the plastic deformation has little been taken into account. The relation of true stress and true strain is based on the assumption of constant volume during tensile deformation. In this paper, solid-state annealing of isotactic polypropylene at high temperature will be adopted to change the crystalline phase only while the amorphous phase keeps nearly intact.[8] Based on this treatment, cavitation, characterized by the volume strain with aid of a CCD camera, will be correlated with the plastic deformation and failure of isotactic polypropylene.

Correspondence to: B. Na (bna@ecit.edu.cn).
Contract grant sponsor: Natural Science Foundation of Jiangxi; contract grant number: 0650009.
Contract grant sponsor: Doctoral Special Foundation of ECIT.

EXPERIMENTAL

Materials and sample preparation

A commercial-grade isotactic polypropylene homopolymer, supplied by Dusanzi Petrolchemical Corp., China, was used as the starting material. It had a weight-average molecular weight M_w of 2.5×10^5 g/mol and M_w/M_n of 3.1. Samples for the mechanical tests were prepared in a hot press with a temperature of 200°C and a pressure of 2 MPa. After 5 min in the press, samples were quickly transferred to a cold press for rapid cooling under a slight pressure. Film thickness was about 0.5 mm. The sample subjected to the above procedure was referred to virgin sample. To obtain the annealed sample, the virgin sample was again placed in the hot press preset at 160°C for 1.5 h and then quenched to room temperature in a cold press.

Differential scanning calorimetry

The thermal analysis of the samples was conducted using a NETZSCH DSC 204, indium calibrated. Melting endotherms were obtained with 6–8 mg of sample at a heating rate of 10°C/min in a nitrogen atmosphere. The enthalpy of melting of 100% crystalline polymer is 177 J/g.[9]

Video-aid tensile tests

Uniaxial tensile tests were performed on the dog-bone samples (4 mm width × 6 mm gauge length) using a universal testing machine (WDT II) equipped with a 200 N load cell at room temperature. To obtain true stress and true strain, a CCD camera (1280 × 1024 pixels), equipped with a tunable magnification lens, was adopted. Its image resolution was 80 pixels/mm. Several grids, one of which had a space of 0.2 mm and 3 mm along axial and transverse direction of dog-bone sample, respectively, were preprinted on the sample with ink. During tensile stretching, the grid that deformed first was monitored by CCD camera and its space change in the axial and transverse direction was simultaneously recorded.

True stress was defined as

$$\sigma = \frac{F}{A} = \frac{F}{A_0} \times \left(\frac{w_0}{w}\right)^2 \tag{2}$$

where F is the transient load, $A_0$the initial cross-sectional area and w_0, w the initial and transient transverse space of the grid, respectively. Note that in eq. (2) transverse isotropy is assumed.[10,11]

True strain was followed Hencky's definition,

$$\varepsilon = \ln\left(\frac{L}{L_0}\right) \tag{3}$$

where L_0, L are the initial and transient space distance of the grid along axial direction, respectively. Moreover, with knowledge of simultaneous space change along axial and transverse direction, the Hencky's volume strain[11] could be obtained as

$$\varepsilon_v = \ln\left(\frac{V}{V_0}\right) = 2\ln\left(\frac{w}{w_0}\right) + \ln\left(\frac{L}{L_0}\right) \tag{4}$$

where V_0, V are the initial and transient volume of the measured grid, respectively.

Impact tensile tests

Impact tensile tests were performed on the double edge-notched sheets with a width of 10 mm at a speed of 500 mm/min,[12] using the above universal testing machine. Notches, perpendicular to the tensile direction, were introduced by a fresh razor blade from both sides. The remaining width of ligament between the notches was about 5 mm. Note that in tensile tests of the samples the deformation was concentrated in the notched regions. The impact energy was calculated by integration of the measured load-displacement curve, divided by the initial cross-sectional area behind the notches. Five specimens were tested for average.

Essential work of fracture tests

Essential work of fracture (EWF) tests were conducted by uniaxial tensile deformation of the deeply double edge-notched samples prepared by cutting the films into rectangular strips with a gauge length of 10 mm and a width of 15 mm. Initial notches were made perpendicularly to the tensile direction with a fresh razor blade. The above procedure for characterization of toughness was referred to the concept of EWF developed recently.[13–15] It had two major advantages: one was that the toughness of ductile polymers could be effectively evaluated due to complete fracture of samples, unlike the situation in common Izod impact tests; the other was that the energy associated with the separation of a crack, which was the intrinsic parameters of samples, could be isolated from the total energy consumed during the deformation. The detailed description of EWF concept can be found elsewhere.[16] In brief, a plot of specific work of fracture w_f, consumed by per unit area of ligament, as a function of ligament length l should be a linear relation. Its interception at zero ligament length and its slope would give the specific essential work of fracture w_e and the specific nonessential work of fracture.βw_p, respectively. For meeting the demands of plane stress and free constraint of boundary, the ligament lengths of specimens were

varied between 2.5 and 5 mm. The ligament lengths were accurately measured at the initial deformation stage with aid of the CCD camera mentioned above. With real time registration of images, it was possible to directly correlate the two dimensional deformation states to the characteristic points of the load-displacement curve. The load-displacement curves were recorded during deformation, and the absorbed energy was calculated by computer integration of the loading curves.

RESULTS AND DISCUSSION

Property of crystalline phase

Figure 1 shows the heating traces of virgin and annealed sample, respectively, at a heating rate of 10°C/min. As for both virgin and annealed sample, there has only one endothermic peak, which is the characteristic of α-form of isotactic polypropylene. The onset melting temperature is about 154°C and 160°C for virgin and annealed sample, respectively. Moreover, the melting temperature increases by about 4°C in the annealed sample. The calculated crystallinity is 0.48 and 0.56 for virgin and annealed sample, respectively. The above differential scanning calorimetry results indicate that upon annealing, the tiny crystallites in the virgin sample have been melted and re-crystallize into thicker lamellae.[8]

Relation of true stress and strain

Figure 2 shows the true stress strain curves of virgin and annealed sample, respectively, at an initial strain rate of 0.005 s^{-1}. Both curves follow the common deformation characteristics of semicrystalline polymers. At the initial stage with a strain less than 0.05, samples deform elastically. The calculated Young's modulus is 1.05 and 1.30 GPa for virgin and annealed sample, respectively. Consistent with the heating traces obtained by differential scanning calorimetry, the increased modulus in annealed sample can be ascribed to the increasing crystallinity and lamellar thickness (deduced from the increasing melting temperature). Subsequently, nonlinear deformation sets in and a strain softening is brought out, which is more severe in the annealed sample. The yield stress is 37.5 and 43.7 MPa for virgin and annealed sample, respectively. Note that the maximum stress around yield is directly taken as yield stress for annealed sample, whereas the determination of yield stress for virgin samples is not straightforward. Therefore, the following definition of yield point is used: the yield point is at the intersection of measured stress-strain curve and a straight line parallel to initial slope of the curve and offset by 2% of strain.[17] In the framework of crystal plasticity, yield is related to the slip of dislocation in the slip plane. Increasing lamellar thickness results in increasing slip resistance and thus enhancing the yield stress, which has been well demonstrated in the literatures.[18–20] On the other hand, yield stress could be related to the crystallinity, which is a long-standing topic in the literatures.[21,22] Increasing crystallinity can reduce the amorphous thickness between adjacent lamellae and thus enhance the coupling of the crystal network, which in turn could be contributed to the increased yield stress in the annealed samples. With increase of strain, plastic flow becomes pronounced after yield, followed by strain hardening until fracture. The fracture stress is lower in the annealed sample, while compared with that of the virgin one.

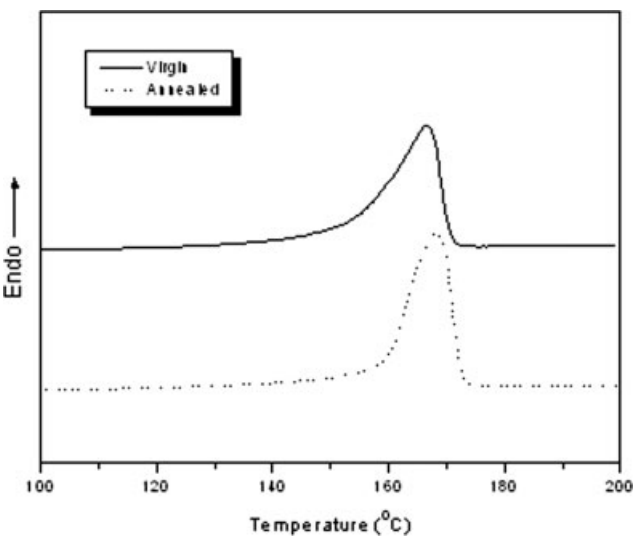

Figure 1 Heating traces of both virgin and annealed samples at a rate of 10°C/min.

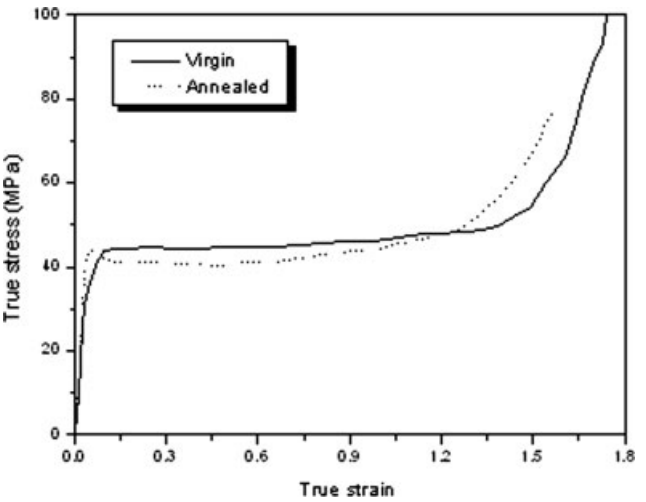

Figure 2 True stress-strain curve of virgin and annealed sample, respectively, at an initial strain rate of 0.005 s^{-1}.

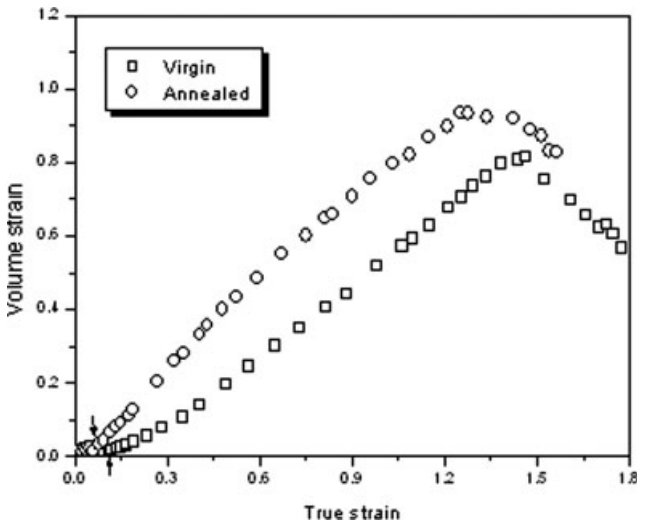

Figure 3 Evolution of volume strain with axial strain under tensile deformation in virgin and annealed sample, respectively, at an initial strain rate of 0.005 s^{-1}. The arrows indicate the onset of steep increasing of volume strain at the second stage.

Evolution of volume strain

During tensile deformation, significant stress whitening is observed in both virgin and annealed samples. It results from the formation of cavities at microscopic scale and can be mostly related to the crystalline phase.[23] Meanwhile, cavitation at microscopic scale can give rise to macroscopic volume dilatation, which can be determined by registering the volume change of the desired grid with aid of a CCD camera. Figure 3 shows the evolution of volume strain with strain for both virgin and annealed samples. Apparently evolution of volume strain for both samples follows the same tendency. In the beginning volume strain increases slightly until yield sets in. With continuing increase of strain to about 1.3 significant increasing of volume strain can be observed at the second stage. Finally volume strain drops at the third stage, which may be resultant from the healing of voids due to reorientation of molecular chains.[24] On the other hand, distinct results can also be observed in both virgin and annealed samples. The strain corresponding to the onset of the second stage, indicated by the arrows in Figure 3, is lower in the annealed sample, which is consistent with the yield strain shown in Figure 2. It again indicates that cavitation in the beginning is accompanied with yield due to competitive relationship between them.[2] Moreover, the volume strain is higher in the annealed sample, while compared with that of virgin one. It can be easily understood because more sites of stress concentration, which trigger the formation and growth of voids, are presented in the annealed sample as a result of higher crystallinity and thicker lamellae.

Failure and toughness

To disclose the effect of cavitation on the failure of isotactic polypropylene, two methods are adopted. One is impact tensile stretching of double edge-notched sample at a crosshead speed of 500 mm/min. Figure 4 shows the typical side-view optical photographs of both virgin and annealed samples after fracture under impact tensile deformation. Few stress whitening outside fracture plane is visible, indication of nearly brittle fracture. The calculated impact strength by integration of load versus displacement is 9.4 and 10.7 N/mm for virgin and annealed sample, respectively.

As suggested by the other method, i.e., EWF concept, the energy absorbed during failure can be divided into two parts. One is the energy associated with the separation of a crack, which is the intrinsic

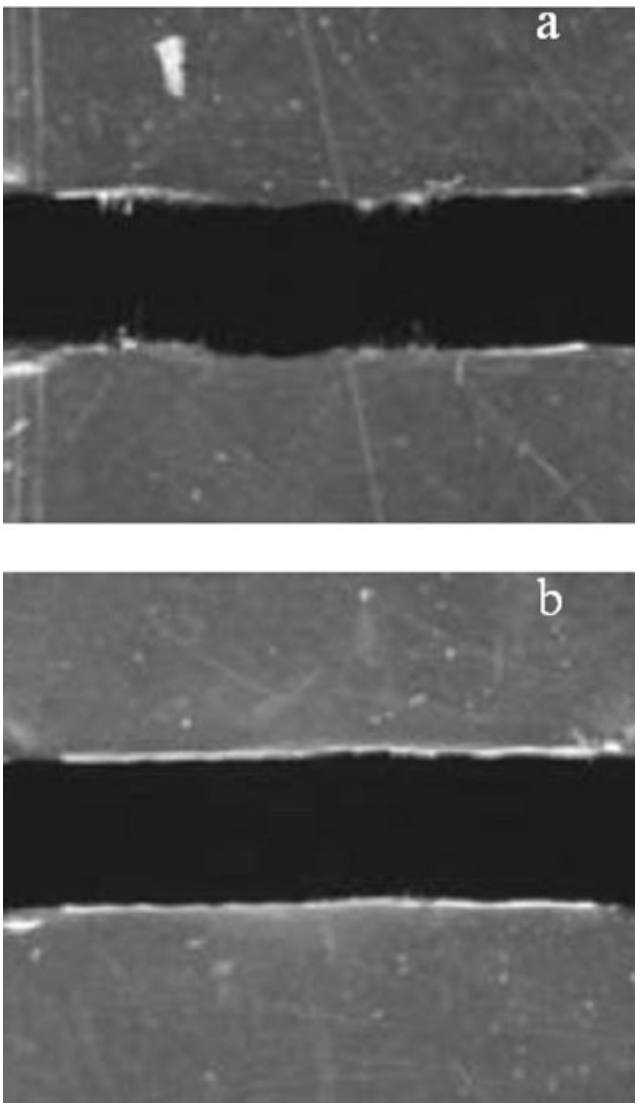

Figure 4 The side-view optical photographs of fractured virgin (a) and annealed (b) samples under impact tensile deformation, respectively.

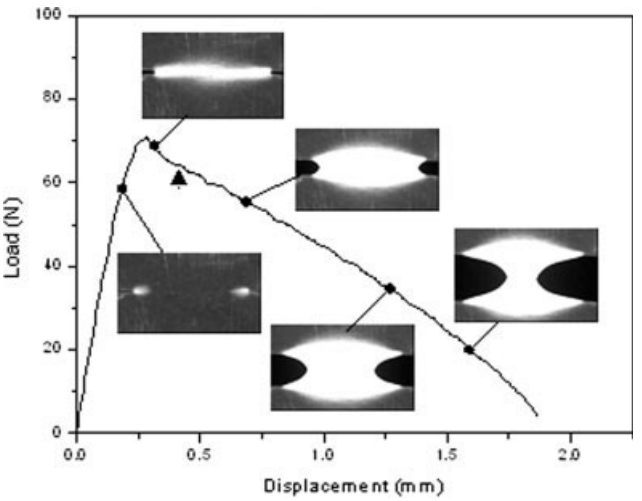

Figure 5 Correlation of two-dimensional states to the stress displacement curves of annealed sample with a ligament length of 4.2 mm at a crosshead speed of 2 mm/min.

parameters of samples, independent of tensile speed. The other is the energy consumed in the outer zone, namely plastic work, which is mostly affected by the loading rate. Based on the above arguments, EWF concept could be more suitable to characterize the toughness of isotactic polypropylene with consideration of its viscoelasticity. Figure 5 shows the typical two dimensional deformation states of deeply double edge-notched specie of annealed sample with a ligament length of 4.2 mm, subjected to tensile deformation at a crosshead speed of 2 mm/min. Note that the arrowhead in Figure 5 denote the onset of crack propagation (see below). Apparently, yield is first initiated from the notches due to stress concentration and stress-whitening zones are formed ahead of notches. With increasing of elongation, stress-whitening zones begin to grow from both sides and then merge into each other. After total yield of whole ligament, crack propagation sets in until the ultimate fracture of samples. With real time registration of ligament width, moreover, the relation of crack growth versus time can be determined. Figure 6 shows, for example, such plots derived from virgin and annealed sample, respectively, with a ligament length of 4.2 mm. Consistent with the results of two-dimensional deformation state, there have two distinct zones during the whole tensile deformation. In the first zone no crack grows, followed by stable crack propagation in the second zone (indication of the arrows in Fig. 6). Moreover, The crack propagation is almost same in both virgin and annealed samples and its growth rate is 0.036 mm/s.

Figure 7 shows the plots of total energy dissipated on per unit area of ligament w_f versus ligament length for both virgin and annealed samples. From the interception of fitted lines at zero ligament length, specific essential work of fracture w_e can be obtained. It is 8.2 and 8.9 N/mm for virgin and annealed sample, respectively. It is evident that the toughness obtained from impact tensile stretching and EWF method, respectively, is very similar. The reason is that in the impact tensile deformation, the energy is mostly consumed to propagate the fracture plane, demonstrated by few stress whitening outside of fracture plane (see Fig. 4), which is exactly the physical meaning of essential work of fracture, w_e.

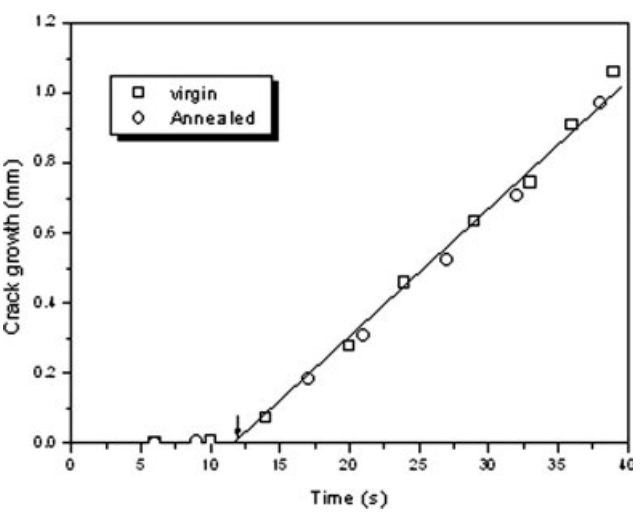

Figure 6 Plots of the crack width versus time for both virgin and annealed samples with a ligament length of 4.2 mm at a crosshead speed of 2 mm/min.

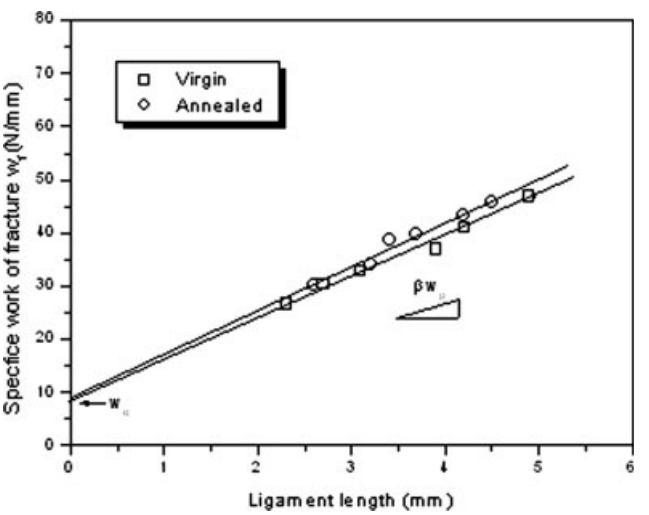

Figure 7 Plots of specific work of fracture w_f as a function of ligament length for both virgin and annealed samples with deeply double edge notches at a crosshead speed of 2 mm/min. Its interception at zero ligament length and its slope would give the specific essential work of fracture w_e, and the specific nonessential work of fracture βw_p, respectively.

Based on the results of volume strain and toughness, it is natural to inspect the effect of cavitation on the failure of isotactic polypropylene. In the literature, it is stated that formation of void can convert plane strain state to plane stress one and thus improve the toughness.[1] In this case, however, void-induced toughening is not obvious, while comparing the results of both virgin and annealed samples. In our viewpoint, the effect of cavitation on the toughness is twofold: one is to induce conversion of stress state and thus promote shear yield; the other is to deteriorate the material due to decreasing of solid fraction.[25] While the above two effects is comparable, little change of toughness can be observed.

CONCLUSIONS

The role of cavitation in the plastic deformation and failure of isotactic polypropylene has been explored with aid of video-aid uniaxial tensile and fracture tests. Macroscopic volume dilatation becomes more severe in the annealed sample, indicating that microscopic cavitation is mostly related to the crystalline phase, since solid-state annealing at 160°C can reserve the amorphous phase nearly intact. In line with the yield strain, moreover, steep increasing of volume strain sets in earlier in the annealed sample. Based on the results of toughness, derived from impact tensile deformation and EWF method, respectively, the effect of cavitation on the failure of isotactic polypropylene has been discussed to some extent.

References

1. Sugimoto, M.; Ishikawa, M; Hatada, K. Polymer 1995, 36, 3675.
2. Pawlak, A.; Galeski, A. Macromolecules 2005, 38, 9688.
3. Duffo, P.; Monasse, B.; Haudin, J. M.; G'Sell, C.; Dahoun, A. J Mater Sci 1995, 30, 701.
4. Li, J. X.; Cheung, W. L.; Chan, C. M. Polymer 1999, 40, 2089.
5. G'Sell, C.; Dahoun, A. Mater Sci Eng A 1994, 175, 183.
6. G'Sell, C.; Hiver, J. M.; Dahouin, A.; Souahi, A. J Mater Sci 1992, 27, 5031.
7. Haward, R. N. Macromolecules 1993, 26, 5860.
8. Schrauwen, B. A. G.; Janssen, R. P. M.; Govaert, L. E.; Meijer, H. E. H. Macromolecules 2004, 37, 6069.
9. Lezak, E.; Bartczak, Z.; Galeski, A. Polymer 2006, 47, 8562.
10. Hiss, R.; Hobeika, S.; Lynn, C.; Strobl, G. Macromolecules 1999, 32, 4390.
11. Addiego, F.; Dahoun, A.; G'Sell, C.; Hiver, J. M. Polymer 2006, 47, 4387.
12. Yang, J.; Zhang, Y.; Zhang, Y. Polymer 2003, 44, 5047.
13. Wu, J.; Mai, Y. W. Polym Eng Sci 1996, 36, 2275.
14. Lach, R.; Schneider, K.; Weidisch, R.; Janke, A.; Knoll, K. Eur Polym J 2005, 41, 383.
15. Karger-Kocsis, J.; Czigany, T.; Moskala, E. J. Polymer 1998, 39, 3939.
16. Ferrer-Balas, D.; Maspoch, M. Ll.; Martinez, A. B.; Santana, O. O. Polymer 2001, 42, 1697.
17. Kazmierczak, T.; Galeski, A.; Argon, A. S. Polymer 2005, 46, 8926.
18. Pluta, M.; Bartczak, Z.; Galeski, A. Polymer 2000, 41, 2271.
19. Kristiansen, M.; Tervoort, T.; Smith, P.; Goossens, H. Macromolecules 2005, 38, 10461.
20. Strobl, G. The Physics of Polymers; Springer: New York, 1997.
21. Men, Y.; Rieger, J.; Strobl, G. Phys Rev Lett 2003, 91, 095502.
22. Men, Y.; Strobl, G. J Macromol Sci Phys B 2001, 40, 775.
23. Men, Y.; Rieger, J.; Homeyer, J. Macromolecules 2004, 37, 9481.
24. Fang, Q. Z.; Wang, T. J.; Li, H. M. Polymer 2006, 47, 5174.
25. Mohanraj, J.; Barton, D. C.; Ward, I. M.; Dahoun, A.; Hiver, J. M.; G'Sell, C. Polymer 2006, 47, 5852.